

53

AM9600009

YERPHI
Preprint YPI-1383(13)-92

ԵՐԵՎԱՆԻ ՖԻԶԻԿԱՅԻ ԻՆՍԻՏՈՒՏ
ЕРЕВАНСКИЙ ФИЗИЧЕСКИЙ ИНСТИТУТ
YEREVAN PHYSICS INSTITUTE

Ts. A. Amatuni, E. A. Mamidjanyan and Kh. N. Sanossyan

Monte-Carlo Simulation of Hadronic Showers

Part 3: The ANI-Prototype Calorimeter

ЦНИИатоминформ
Ереван 1982

VOL 27 № 22



Центральный научно-исследовательский институт информации
и технико-экономических исследований по атомной науке
и технике (ЦНИИатоминформ) 1992 г.

1. The experimental setup

The ANI-Prototype is one of the components of the ANI-facility[1-3] on mountain Aragads. It was constructed in order to develop in practice the combination of three detection techniques: X-ray films, ionization chambers and scintillation counters in order to simulate the central overground part of the ANI facility and to study the characteristics of multycore EAS [4,5].

The hadron-photon experimental facility consists of two parts: the hadronic module (ANI-Prototype calorimeter) and the EAS detector [6] (scintillator array [7] and hodoscope system [8,9]). The schematic layout of the ANI-Prototype calorimeter is presented in figure 3.1. The scintillator rows are not installed yet. The sequence of materials of calorimeter layers used for the present simulation is given in Table 3-1. As it is seen from the table the overall depth of the absorbers is $Z_{max}=226.2\text{cm}$ and amounts to $\sim 278\text{g/cm}^2$. The area of the calorimeter is $6\times 40\text{m}^2$ (the module length equals 40m and is defined from the constructive specifications of the ANI-facility [1-3, 10]).

The ANI-Prototype calorimeter is covered from the top by 3cm lead and 2.5mm iron plates under which the modules of proportional chambers have to be arranged 3m long and 40cm wide[11]. The axes of the proportional wire chambers, which will be arranged within the two upper gaps, are perpendicular, and 3cm lead plate is interleaved between them. This part of the setup allows to investigate the spatial distribution of the energy flux of the EAS electromagnetic component.

Further the 45cm thick carbon absorber is installed which amounts to about one nuclear interaction length. There is a 4.5cm thick lead plate under the carbon absorber bellow which two layers of PT-6M type X-ray films are installed. The upper X-ray film layer is fixed, the lower layer can be moved along the longer side of the setup by the help of a specialized belt pulling gear. Each layer of X-ray film

consists of 11 strips 42cm wide placed within light-proof gaps.

X-ray films, with the absorber above them, form the hadronic X-ray chambers, which are similar to those used in experiment "Pamir" [12], and those to be used in the "ANI" experiment [1-3,13]. The method of treatment of X-ray films developed in ref. [14] makes it possible to compare the results of three experiments "Pamir", "ANI-Prototype" and "ANI".

Two rows of ionization chambers follow the X-ray films [15]. Twenty 40m long chambers and 130 5m long chambers are installed in the upper and lower rows respectively. There is a 6cm thick lead plate between the two rows of ionization chambers. The IC-s were manufactured of galvanized 5m long iron tubes, having 2mm wall thickness and 250mm internal diameter. The tubes can be hermetically joined to make chambers of arbitrary length (multiple of 5m). The IC-s are filled with argon at 3 atm. The anode is made of a 6mm copper-nickel alloy tube with 0.4mm wall thickness (see ref.-s [10,15]).

2. The Monte-Carlo Simulation

The Monte-Carlo simulations of the calorimeter were carried out with the help of the MARS10 code [16-18]. The simulations for incident energies above 20TeV were carried out by using the same interaction cross sections as for 20TeV. The simulations were performed in cylindrical geometry with the Z-axis pointed downwards and the origin at the middle of the calorimeter upper surface. The energy cutoff was 10MeV. The number of simulated showers per each primary was 10000. The primary protons were incident along the Z-axis. Hadron cascades were calculated for 0.5, 1, 2, 4, 5, 7, 10, 12, 15, 20,22 and 30TeV primary energies.

The energy dependence of the total energy deposition in the calorimeter is presented in figure 3.2. It can be fitted by the following relationship:

$$E_{\text{tot}} = 0.63(\pm 0.09) \cdot E_0^{0.91(\pm 0.02)}, \quad (E_{\text{tot}} \text{ and } E_0 \text{ in GeV}). \quad (3.1)$$

The energy dependence of the energy deposition in argon layers (the "detected" energy in ionization chambers) of the calorimeter is presented in figure 3.3. It can be fitted by the following formula:

$$E_{Ar}(\text{MeV}) = 0.5(\pm 0.3) \cdot E_0^{0.96(\pm 0.07)}, \quad (E_0 \text{ in GeV}). \quad (3.2)$$

The departure from linearity in eq.-s (3.1) and (3.2) is a consequence of substantial energy leakage.

The longitudinally integrated (over the calorimeter length) reduced lateral profiles -

$$1/E_{tot}(\Delta E_{tot}/\Delta R),$$

where

E_{tot} - is the total deposited energy,

ΔE_{tot} - is the energy deposited in a cylindrical ring of ΔR thickness and Z_{max} height, are presented in figure 3.4. The reduced lateral energy depositions in the two argon layers of the calorimeter for 0.5, 5 and 20TeV proton induced showers are presented respectively in figures 3.5, 3.6 and 3.7. These can be fitted by the following exponential formula:

$$f(R) = 1/E_{Ar}(\Delta E_{Ar}/\Delta R) = N_T(p/2) \exp(-r^p pR), \quad (3.3)$$

where

R - is the distance from the shower axis,

E_{Ar} - is the sum of the energy depositions in the two argon layers,

ΔE_{Ar} - is the energy deposited within $[R, R+\Delta R]$ in the two argon layers,

p - is the shape parameter,

N_T - is fixed by the normalization condition

$$\int f(R) dR = E_{Ar}, \quad (3.4)$$

giving

$$N_T = E_{Ar}. \quad (3.5)$$

The shape parameter p is obtained from a χ^2 - fit to the Monte-Carlo points with

$$\chi^2 = \sum [(1/E_0)(\Delta E/\Delta R) - (1/R) \int_R^{R+\Delta R} f(R) dR]^2 / \sigma^2. \quad (3.6)$$

The χ^2 - minimization was performed by MINUIT[19].

The energy dependence of the fitted values of the slope parameter are listed in Table 3.2. As it is seen from the table there is no energy dependence of p within the error limits and it can be approximated by

$$p \approx 0.30 \pm 0.04. \quad (3.7)$$

The leakage energy and the number of leakage particles for 0.5, 1, 2, 4, 5, 7, 10, 12, 15, 20, 22, 30 TeV proton induced showers are listed in Table 3.3. The energy dependence of the forward leakage energy is given in figure 3.8. It can be fitted by the formula:

$$E_L = 0.69(\pm 0.003) E_0^{0.993(\pm 0.0004)}, \quad (E_L \text{ and } E_0 \text{ in GeV}). \quad (3.8)$$

The energy dependence of the number of forward leakage particles is given in figure 3.9. It can be fitted by the formula:

$$N_L = 1.91(\pm 0.04) E_0^{0.576(\pm 0.002)}, \quad (E_0 \text{ in GeV}). \quad (3.9)$$

Conclusions and acknowledgements

Formula (3.2) can be used for estimating the primary energy by measuring the ionization in the active absorber rows. Formula (3.3) is useful for the estimation of the shower lateral dimensions and for the decision of optimum lateral segmentation in the ANI calorimeter.

We would like to thank Dr.-s. V. Avakyan and G. Avakyan for numerous discussions and interest in this work. We would like to thank Dr.-s. N. Mokhov and A. Uzunyan from JHEP(Serpukhov) who made available for us the 10-th version of JHEP code.

TABLES

Table 3-1. The sequence of materials with corresponding thickness and density in the ANI-Prototype calorimeter.

Depth cm	ΔZ g/cm^2	$p\Delta Z$ cm	$p\Delta Z$ g/cm^2	Medium
3.	34.05	3.	34.05	Pb
3.25	36.0175	0.25	1.9675	Fe
10.25	36.0265	7.	0.00903	Air
20.25	36.0394	10.	0.0129	Air
23.25	70.0894	3.	34.05	Pb
39.25	70.1101	16.	0.02064	Air
49.25	70.123	10.	0.0129	Air
74.25	70.1552	25.	0.03225	Air
119.25	147.1052	45.	76.95	C
123.75	198.1802	4.5	51.075	Pb
126.25	198.1834	2.5	0.003225	Air
126.5	200.1459	0.25	1.9625	Fe
150.5	200.1769	24.	0.03096	Air
150.8	202.5379	0.3	2.361	Fe
175.8	202.6714	25.	0.1335	Ar
176.1	205.0324	0.3	2.361	Fe
183.1	205.0414	7.	0.00903	Air
187.1	205.0466	4.	0.00516	Air
193.1	273.1466	6.	68.1	Pb
200.6	273.1563	7.5	0.009675	Air
200.9	275.5173	0.3	2.361	Fe
225.9	275.6508	25.	0.1335	Ar
226.2	276.0116	0.3	2.361	Fe

Table 3-2. The energy dependence of the slope parameter in formula (3.3).

E_0, TeV	p	Δp
0.5	0.25	0.02
5.	0.26	0.03
20.	0.34	0.04

Table 3-3. Leakage from the ANL-Prototype calorimeter.
 (Number of showers is 10000, hadron cutoff energy is 10MeV.)

Incident Energy, TeV	Leakage			Energy, GeV			Number of Leakage Particles			
	Hadrons			Low- Energy	Photons and Neutrons	Total Electrons	Backward	Forward	Side	Total
	Backward	Forward	Side							
0.5	0.46	327.	0.50	0.03	38.	366.	5.	67.	6.	78.
1.	0.23	644.	0.73	0.05	91.	736.	4.	102.	9.	115.
2.	0.18	1293.	1.16	0.07	216.	1511.	4.	153.	14.	171.
4.	0.16	2599.	1.28	0.09	505.	3106.	4.	248.	16.	268.
5.	0.18	3231.	1.16	0.07	673.	3906.	4.	261.	19.	284.
7.	0.34	4542.	1.95	0.08	1025.	5569.	7.	308.	30.	345.
10.	0.44	6486.	3.12	0.11	1572.	8061.	9.	368.	37.	414.
12.	0.80	7844.	3.45	0.15	2019.	9868.	21.	477.	48.	546.
15.	0.47	9680.	2.31	0.13	2605.	12290.	10.	445.	35.	490.
20.	0.32	12830.	2.43	0.12	3698.	16530.	7.	590.	31.	628.
22.	0.32	14490.	2.44	0.26	4333.	18830.	7.	578.	34.	619.
30.	0.42	19340.	5.62	0.23	6011.	25360.	10.	749.	67.	826.

ANI - PROTOTYPE CALORIMETER

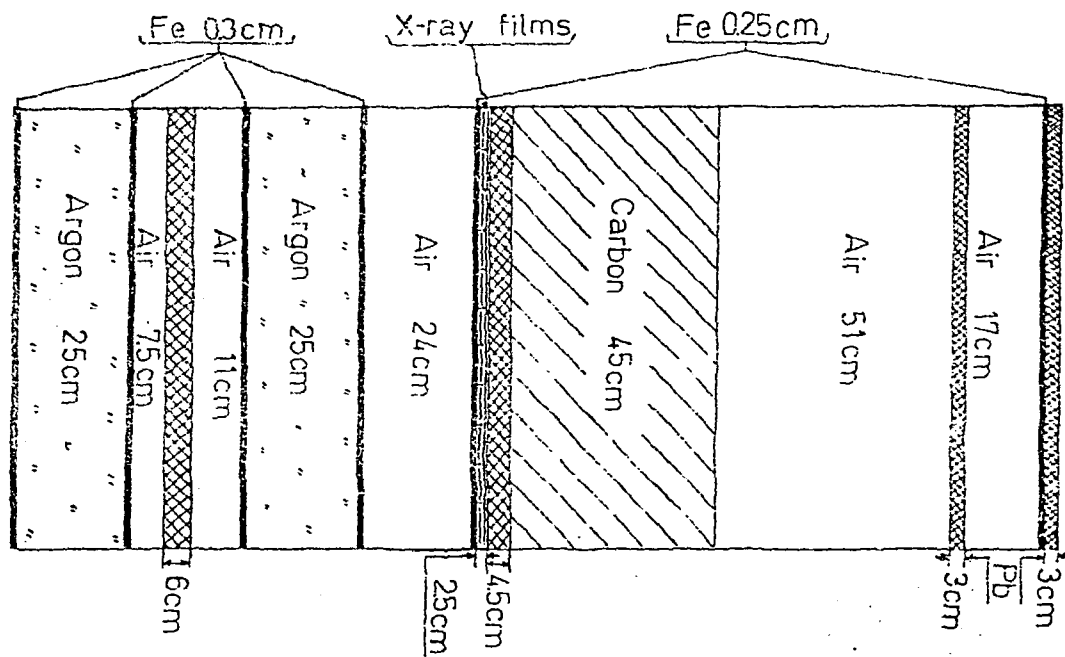


Fig. 3.1

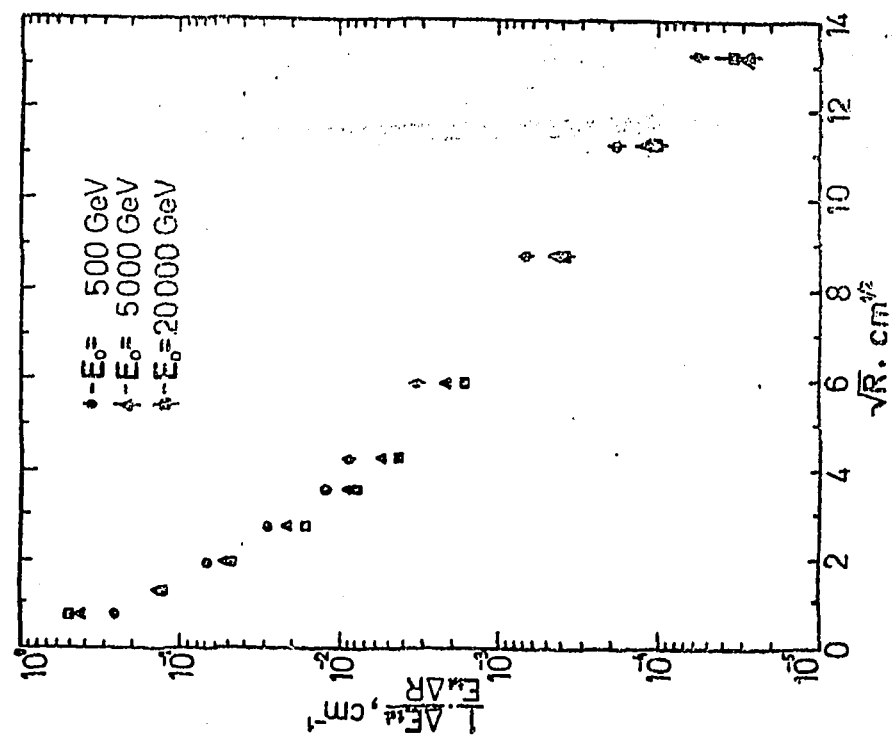


Fig. 3.3

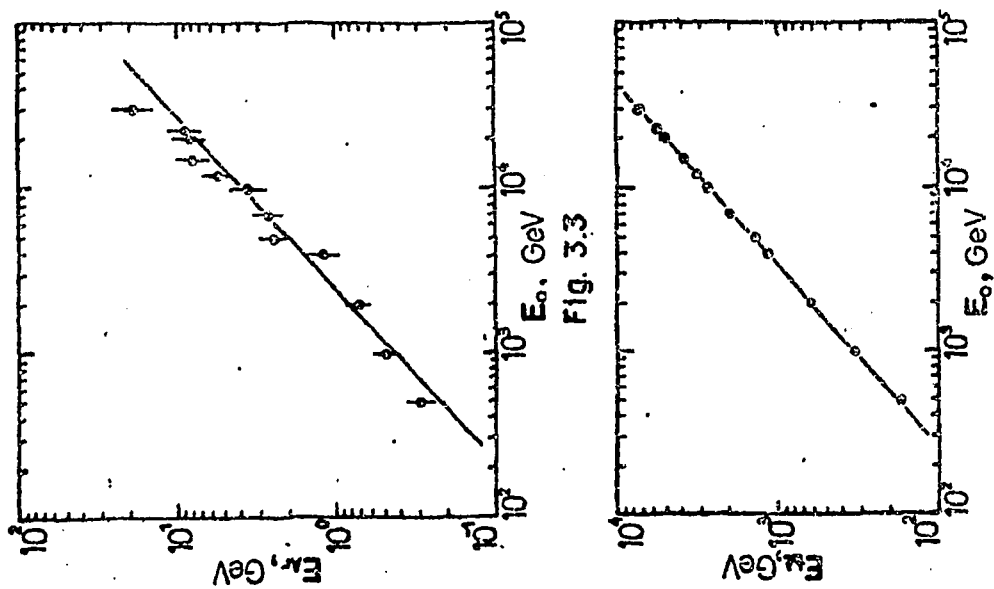


Fig. 3.2

Fig. 3.4

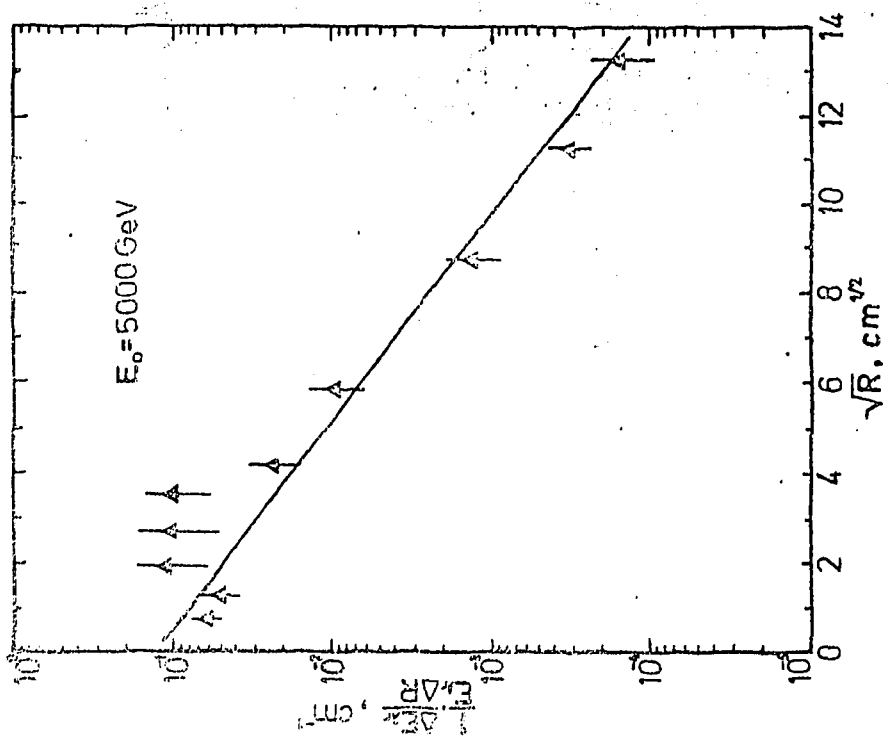


Fig. 3.6

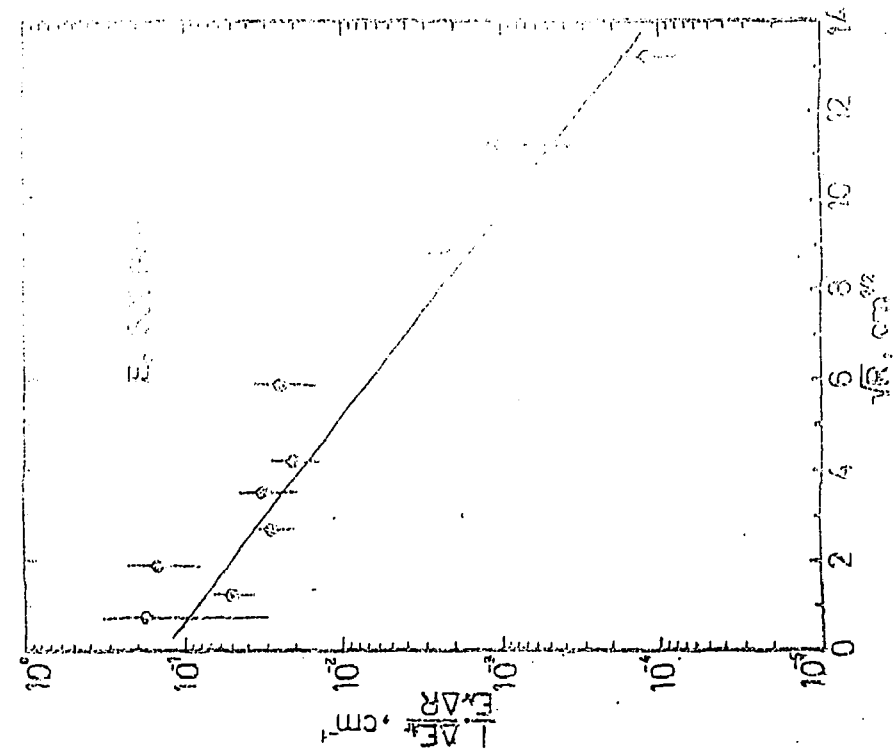


Fig. 3.5

POOR QUALITY
ORIGINAL

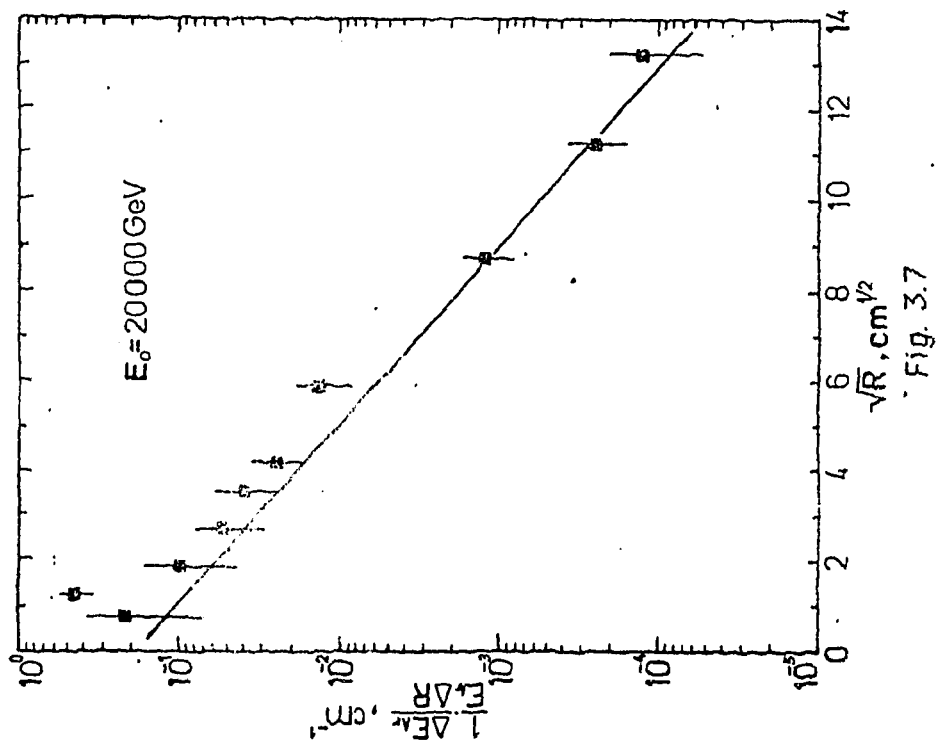
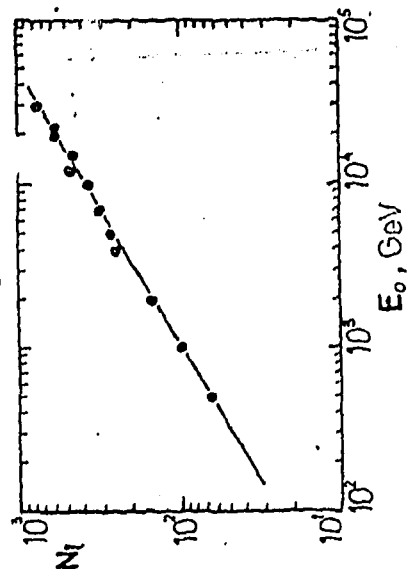
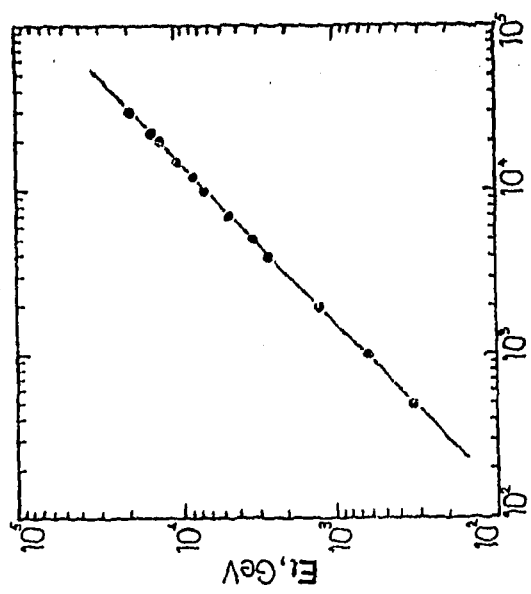


FIGURE CAPTIONS

Fig. 3.1. The layout of the ANI-Prototype calorimeter.

Fig. 3.2. Dependence of total energy deposition on primary energy.
• - MARS10, — — fit (formula (3.1)).

Fig. 3.3. Dependence of energy deposition in argon on primary energy. • - MARS10, — — fit (formula (3.2)).

Fig. 3.4. Reduced lateral shower profiles in ANI-Prototype calorimeter. E_0 - is the incident energy.

Fig. 3.5. Reduced lateral shower profile in the ionization chambers (in Ar) of the calorimeter for $E_0 = 500\text{GeV}$. • - MARS10,
— — fit (formula (3.3)).

Fig. 3.6. The same as in fig. 3.5 for $E_0 = 5000\text{GeV}$. • - MARS10,
— — fit (formula (3.3)).

Fig. 3.7. The same as in fig. 3.5 for $E_0 = 20000\text{GeV}$. • - MARS10,
— — fit (formula (3.3)).

Fig. 3.8. Dependence of the forward leakage energy on primary energy. • - MARS10, — — fit (formula (3.8)).

Fig. 3.9. Dependence of the number of forward leakage particles on primary energy. • - MARS10, — — fit (formula (3.9)).

REFERENCES

- [1] A. Ts. Amatuni, E. A. Mamidjanyan, S. H. Matinyan et al., Preprint YPI-358(16)-79, Yerevan, 1979 (in Russian).
- [2] Yerevan-Lebedev Physics Institute collaboration, Izvestiya AN Arm. SSR, Fizika, 17 (3-4), 129-232, Yerevan, 1982 (in Russian).
- [3] E. A. Mamidjanyan and S. I. Nikolski, Preprint YPI-1301(87), Yerevan, 1990 (in Russian).
- [4] V. V. Avakyan et al., VANT, Seriya: TPE, 5(31), 3 (1988) (in Russian).
- [5] V. V. Avakyan et al., Proc. of the 21-st ICRC, v. 10, 162 (1990).
- [6] N. V. Kabanova, V. A. Romakhin, Preprint Lebedev Phisics Institute, #65, Moscow, 1990 (in Russian).
- [7] V. V. Avakyan, S. A. Arzumanyan, G. A. Baghdasaryan, VANT, Seriya: TPE, 3(20), 69 (1984) (in Russian).
- [8] G. Ds. Avakyan, K. M. Avakyan, K. G. Sahakyan, VANT, Seriya: TPE, 4(25), 90 (1985) (in Russian).
- [9] G. Ds. Avakyan and K. M. Avakyan, VANT, Seriya: TPE, 5(17), 5, (1983) (in Russian).
- [10] G. Ds. Avakyan, Thesis, Yerevan Physics Institute, 1990.
- [11] E. V. Bazarov, S. Yu. Grigoriev, E. V. Danilova et al., VANT, Seriya: TPE, 5(31), 3 (1986) (in Russian).
- [12] S. G. Baibourina, A. S. Borisov, Z. M. Gouseva et al., Proc. of Lebedev Phisics Institute, v. 154, 3-217, Moscow, 1984 (in Russian).
- [13] Ts. A. Amatuni, E. A. Mamidjanyan and Kh. N. Sanossyan, Part 4 of this work and ref.-s therein. Preprint YPI-1384(14)-92, Yerevan, 1992.
- [14] L. G. Melkoumyan, Thesis, Yerevan Physics Institute, 1990.

[15] G. Ds. Avakyan, K. M. Avakyan, P. S. Mnatsakanyan et al., Proc. of the IC, Praha, p.167, 1989.

[16] A. N. Kalinowski, N. V. Mokhov and Yu. P. Nikitin, Passage of High Energy Particles Through Matter, Energoatomizdat, Moscow, 1985 (In Russian).

[17] N. V. Mokhov and J. D. Cossairt, Fermilab Report, FN-424, 1985.

[18] Ts. A. Amatuni, E. A. Mamidjanyan and Kh. N. Sanossyan, Part 1 of this work. Preprint YPI-1381(11)-92, Yerevan, 1992.

[19] CERN Program Library.

The manuscript was received 13th Oct. 1992

The address for requests:
Information Department
Yerevan Physics Institute
Alikhanian Brothers 2,
Yrevan, 375036
Armenia, USSR

Ц.А.АМАТУНИ, Э.А.МАМИДЖАНЯН, Х.Н.САНОСЯН

МОДЕЛИРОВАНИЕ АДРОННЫХ ЛИВНЕЙ МЕТОДОМ МОНТЕ-КАРЛО
ЧАСТЬ 3: КАЛОРИМЕТР УСТАНОВКИ "АНИ-Макет"

(на английском языке)

Редактор А.С.Есин

Технический редактор А.С.Абрамян

Подписано в печать 5 /ХII-92г.

Формат 60x84x16

Офсетная печать. Уч.изд.л. 1,0

Тираж 100 экз. ц. 8 р.

Зак.тип.064

Индекс 3649

Отпечатано в Ереванском физическом институте

Ереван-36, ул.Братьев Алиханян, 2

ИНДЕКС 3649



ЕРЕВАНСКИЙ ФИЗИЧЕСКИЙ ИНСТИТУТ